Supporting Information

for

Single Molecule Magnetism in a family of mononuclear β-diketonate lanthanide(III) complexes: rationalization of magnetic anisotropy in complexes of low symmetry

Nicholas F. Chilton,[a] Stuart K. Langley,[a] Boujemaa Moubaraki,[a] Alessandro Soncini,[b] Stuart R. Batten[a] and Keith S. Murray[a]*

[a] School of Chemistry, Monash University, Clayton, Victoria 3800, Australia

[b] School of Chemistry, University of Melbourne, Parkville, Victoria 3010, Australia

1. Experimental

General

All reactions were carried out under aerobic conditions. All chemicals and solvents were obtained from commercial sources and used without further purification, except the ligand paaH which was prepared according to the literature.[1]

Microanalysies were carried out by Campbell Microanalytical Laboratory, University of Otago, Dunedin, New Zealand.

IR spectra were recorded as neat samples on a Bruker Equinox 55 spectrometer fitted with an ATR sampler from Specac Inc.

DC and AC magnetic measurements were conducted using a Quantum Design MPMS-XL 7 SQUID magnetometer. Microcrystalline samples were dispersed in Vaseline to avoid torquing of the crystallites. These sample mulls were contained in a calibrated gelatin capsule held at the centre of a drinking straw that was fixed at the end of the sample rod. DC measurements used fields from 0 – 5 T and temperatures of 1.8 – 300 K. AC measurements used an oscillating field of 3 Oe and frequencies from 0.1 – 1500 Hz.

X-Ray crystallographic measurements for **1**, **5**, **7**, **9**, **10** and **11** were performed at 123(2) K using a Bruker Smart Apex X8 diffractometer with Mo-Kα radiation. The data collection and integration were performed within SMART and SAINT+ software programs and corrected for absorption using the Bruker SADABS program.[2] X-ray crystallographic measurements for **2**, **3**, **4**, **6** and **8** were performed at 100(2) K at the Australian synchrotron MX1 or MX2 beamlines. The data collection and integration were performed within Blu-Ice[3] and XDS[4] software programs. All compounds were solved by direct or Patterson methods (SHELXS-97) and refined (SHELXL-97) by full least matrix least-squares on all F^2 data.[5] Compounds **2-4**, **6**, **7** and **9** suffered from low data completeness, in most cases due to the single-axis geometry of the MX1 and MX2 diffractometers. Thus bond lengths and angles should be treated with caution, although the connectivity in these structures is unambiguous, particularly given that they are all part of isomorphous series. Crystallographic data and refinement parameters for all compounds are summarized in Tables S1 – S4. CCDC numbers 914618 to 914691. These data can be obtained free of charge from the Cambridge Crystallographic Data Centre via www.ccdc.cam.ac.uk/data_request/cif.

Syntheses

$[Gd(paaH^*)_2(H_2O)_4][Cl]_3 \cdot 2H_2O$ (1)

$GdCl_3.6H_2O$ (0.666 g, 1.8 mmol) and paaH (0.890 g, 5.0 mmol) in slight excess were each dissolved independently in ~ 5mL of MeOH and these solutions heated to boiling point dissolve the starting materials. Upon complete dissolution, the two solutions were combined and held at boiling point. The pH of the reaction was monitored with a pH meter while HCl (1 mL 32% HCl : 9 mL MeOH) was added slowly to lower the pH to ~ 0.5 (~ 2.46 mL, 2.5 mmol HCl). The solution was then removed from the heat and to it was added enough diethyl ether to change the colour from transparent yellow to opaque white (~ 50 mL). This suspension was allowed to stand, at which point a yellow oil gathered at the bottom of the flask. The oil was collected, redissolved in methanol and left to allow evaporation of the solvent. Crystals suitable for XRD studies were obtained within 3 to 7 days. **Yield** 200 mg (15 %); **IR (cm^{-1})** 3323 (br, w), 1654 (sh, s), 1611 (sh, s), 1567 (sh, w), 1511 (sh, s), 1462 (sh, s), 1430 (sh, s), 1406 (sh, s), 1379 (sh, m), 1244 (sh, m), 1180 (sh, w), 1160 (sh, m), 970 (sh, m), 765 (sh, w); **Microanalysis** % found (calc for $GdC_{18}H_{32}N_4Cl_3O_{10}$) C 30.4 (29.69), H 4.40 (4.43), N 7.72 (7.70); **MP** 208 – 216 °C (dec).

$[Tb(paaH^*)_2(H_2O)_4][Cl]_3 \cdot 2H_2O$ (2)

Preparation as for **1**, but $TbCl_3.6H_2O$ (0.670 g, 1.8 mmol) used in place of $GdCl_3.6H_2O$. **Yield** 210 mg (16 %); **IR (cm^{-1})** 3350 (br, w), 1654 (sh, s), 1609 (sh, s), 1564 (sh, w), 1512 (sh, s), 1461 (sh, s), 1430 (sh, s), 1405 (sh, s), 1374 (sh, m), 1245 (sh, m), 1179 (sh, w), 1160 (sh, m), 970 (sh, m), 768 (sh, w); **Microanalysis** % found (calc for $TbC_{18}H_{32}N_4Cl_3O_{10}$) C 29.4 (29.63), H 4.5 (4.42), N 7.53 (7.68); **MP** 217 – 222 °C (dec).

$[Dy(paaH^*)_2(H_2O)_4][Cl]_3 \cdot 2H_2O$ (3)

Preparation as for **1**, but $DyCl_3.xH_2O$ (0.675 g, ~ 1.8 mmol) used in place of $GdCl_3.6H_2O$. **Yield** 205 mg (16 %); **IR (cm^{-1})** 3305 (br, w), 1653 (sh, s), 1612 (sh, s), 1566 (sh, w), 1511 (sh, s), 1462 (sh, s), 1430 (sh, s), 1404 (sh, s), 1376 (sh, m), 1248 (sh, m), 1179 (sh, w), 1158 (sh, m), 970 (sh, m), 767 (sh, w); **Microanalysis** % found (calc for $DyC_{18}H_{32}N_4Cl_3O_{10}$) C 28.14 (29.48), H 4.11 (4.40), N 7.18 (7.64); **MP** 217 – 222 °C (dec).

$[Ho(paaH^*)_2(H_2O)_4][Cl]_3 \cdot 2H_2O$ (4)

Preparation as for **1**, but $HoCl_3.6H_2O$ (0.681 g, 1.8 mmol) used in place of $GdCl_3.6H_2O$ and an orange oil was recovered. **Yield** 192 mg (14 %); **IR (cm^{-1})** 3313 (br, w), 1653 (sh, s), 1611

(sh, s), 1565 (sh, m), 1512 (sh, m), 1463 (sh, s), 1430 (sh, s), 1406 (sh, s), 1375 (sh, m), 1249 (sh, m), 1179 (sh, w), 1158 (sh, m), 972 (sh, m), 766 (sh, m); **Microanalysis** % found (calc for $HoC_{18}H_{32}N_4Cl_3O_{10}$) C 29.20 (29.38), H 4.38 (4.38), N 7.48 (7.61) , **MP** 210 – 217 °C (dec).

$[Er(paaH^*)_2(H_2O)_4][Cl]_3 \cdot 2H_2O$ (5)

Preparation as for **1**, but $ErCl_3.xH_2O$ (0.684 g, ~ 1.8 mmol) used in place of $GdCl_3.6H_2O$ and a pink oil was recovered. **Yield** 270 mg (20 %); **IR (cm^{-1})** 3295 (br, m), 1656 (sh, m), 1613 (sh, s), 1567 (sh, m), 1516 (sh, s), 1467 (sh, s), 1433 (sh, m), 1408 (sh, s), 1377 (sh, s), 1248 (sh, s), 1181 (sh, w), 1156 (sh, s), 973 (sh, m), 768 (sh, m); **Microanalysis** % found (calc for $ErC_{18}H_{32}N_4Cl_3O_{10}$) C 28.68 (29.29), H 4.57 (4.37), N 7.43 (7.59); **MP** 212 – 218 °C (dec).

$[Y(paaH^*)_2(H_2O)_4][Cl]_3 \cdot 2H_2O$ (6)

Preparation as for **1**, but $YCl_3.xH_2O$ (0.546 g, ~ 1.8 mmol) used in place of $GdCl_3.6H_2O$. **Yield** 230 mg (19 %); **IR (cm^{-1})** 3325 (br, w), 1653 (sh, s), 1611 (sh, s), 1566 (sh, w), 1511 (sh, s), 1462 (sh, s), 1429 (sh, s), 1405 (sh, s), 1374 (sh, m), 1249 (sh, m), 1178 (sh, w), 1156 (sh, m), 970 (sh, m), 765 (sh, w); **Microanalysis** % found (calc for $YC_{19}H_{24}N_7O_{14}$) C 33.8 (32.77), H 4.80 (4.89), N 8.81 (8.49); **MP** 230 – 240 °C (dec).

$[Tb(paaH^*)_2(NO_3)_2(MeOH)][NO_3]$ (7)

$Tb(NO_3)_3.5H_2O$ (0.217 g, 0.5 mmol) and paaH (0.178 g, 1.0 mmol) were each dissolved independently in ~ 5mL of MeOH and these solutions heated to dissolve the starting materials. Upon complete dissolution the solutions were combined and removed from the heat. This mixture was then left in a sample vial with no lid to allow evaporation of the solvent. Yellow single crystals suitable for XRD were obtained on the top edge of the vial within 3 to 5 days. The bulk sample was thoroughly washed until clear with cold acetone, followed by washings with cold MeOH and Et_2O. **Yield** 143 mg (39 %); **IR (cm^{-1})** 3237 (sh, w), 2983 (br, w), 1659 (sh, s), 1630 (sh, m), 1607 (sh, m), 1563 (sh, m), 1516 (sh, m), 1462 (sh, s), 1433 (sh, s), 1406 (sh, m), 1368 (sh, m), 1295 (sh, s), 1276 (sh, m), 1244 (sh, m), 1183 (sh, m), 1158 (sh, s), 1047 (sh, w), 1021 (sh, m), 1000 (sh, w), 968 (sh, m), 913 (br, w), 793 (sh, w), 770 (sh, m), 738 (sh, w); **Microanalysis** % found (calc for $TbC_{19}H_{24}N_7O_{14}$) C 31.02 (31.12), H 3.20 (3.30), N 13.27 (13.37); **MP** 160 – 165 °C.

$[Dy(paaH^*)_2(NO_3)_2(MeOH)][NO_3]$ (8)

Preparation as for **7**, but $Dy(NO_3)_3.5H_2O$ (0.180 g, 0.4 mmol) used in place of $Tb(NO_3)_3.5H_2O$. **Yield** 121 mg (33 %); **IR (cm^{-1})** 3237 (sh, w), 2979 (br, w), 1659 (sh, s), 1630 (sh, m), 1607 (sh, m), 1563 (sh, m), 1516 (sh, m), 1462 (sh, s), 1433 (sh, s), 1407 (sh, m), 1369 (sh, m), 1296 (sh, s), 1277 (sh, m), 1244 (sh, m), 1183 (sh, m), 1158 (sh, s), 1047 (sh, w), 1021 (sh, m), 1000 (sh, w), 969 (sh, m), 914 (br, w), 793 (sh, w), 769 (sh, m), 739 (sh, w); **Microanalysis** % found (calc for $DyC_{19}H_{24}N_7O_{14}$) C 30.77 (30.97), H 3.28 (3.28), N 13.12 (13.30); **MP** 163 – 167 °C.

$[Ho(paaH^*)_2(NO_3)_2(MeOH)][NO_3]$ (9)

Preparation as for **7**, but $Ho(NO_3)_3.5H_2O$ (0.220 g, 0.5 mmol) used in place of $Tb(NO_3)_3.5H_2O$ and orange crystals were obtained. **Yield** 136 mg (37 %); **IR (cm^{-1})** 3240 (sh, w), 2982 (br, w), 1662 (sh, s), 1632 (sh, m), 1609 (sh, m), 1565 (sh, m), 1519 (sh, m), 1466 (sh, s), 1436 (sh, s), 1409 (sh, m), 1371 (sh, m), 1300 (sh, s), 1279 (sh, m), 1247 (sh, m), 1185 (sh, m), 1161 (sh, s), 1049 (sh, w), 1023 (sh, m), 1002 (sh, w), 971 (sh, m), 917 (br, w), 795 (sh, w), 772 (sh, m), 748 (sh, w); **Microanalysis** % found (calc for $HoC_{19}H_{24}N_7O_{14}$) C 30.77 (30.87), H 3.06 (3.27), N 13.19 (13.26); **MP** 160 – 165 °C.

$[Er(paaH^*)_2(NO_3)_2(MeOH)][NO_3]$ (10)

Preparation as for **7**, but $Er(NO_3)_3.5H_2O$ (0.222 g, 0.5 mmol) used in place of $Tb(NO_3)_3.5H_2O$ and pink crystals were obtained. **Yield** 116 mg (31 %); **IR (cm^{-1})** 3238 (sh, w), 2973 (br, w), 1660 (sh, s), 1631 (sh, m), 1607 (sh, m), 1564 (sh, m), 1517 (sh, m), 1464 (sh, s), 1434 (sh, s), 1408 (sh, m), 1369 (sh, m), 1298 (sh, s), 1277 (sh, m), 1245 (sh, m), 1183 (sh, m), 1159 (sh, s), 1047 (sh, w), 1022 (sh, m), 1000 (sh, w), 969 (sh, m), 916 (br, w), 793 (sh, w), 769 (sh, m), 747 (sh, w); **Microanalysis** % found (calc for $ErC_{19}H_{24}N_7O_{14}$) C 30.82 (30.77), H 3.12 (3.26), N 13.12 (13.22); **MP** 160 – 165 °C.

$[Y(paaH^*)(NO_3)_3(H_2O)]$ (11)

Preparation as for **7**, but $Y(NO_3)_3.xH_2O$ (0.200 g, ~ 0.5 mmol) used in place of $Tb(NO_3)_3.5H_2O$. Following evaporation of the MeOH, a yellow oil was obtained and re-dissolved in MeCN. A slow evaporation of this solution led to the formation of **11**. **Yield** < 5 mg (< 2 %); **IR (cm^{-1})** 3505 (sh, w), 1692 (sh, m), 1655 (sh, m), 1630 (sh, s), 1610 (sh, s), 1570 (sh, m), 1518 (sh, s), 1455 (sh, s), 1441 (sh, s), 1408 (sh, m), 1363 (sh, m), 1318 (sh, m), 1275 (sh, m), 1251 (sh, m), 1181 (sh, m), 1164 (sh, m), 1152 (sh, m), 1053 (sh, m), 1026

(sh, m), 966 (sh, m), 887 (sh, w), 80 (sh, m), 763 (sh, m); **Microanalysis** insufficient sample; **MP** insufficient sample.

2. X-Ray crystallography

Table S1 – X-ray crystallographic data for 1 – 3.

	1	2	3
Formula	$C_{18}H_{32}Cl_3N_4O_{10}Gd$	$C_{18}H_{32}Cl_3N_4O_{10}Tb$	$C_{18}H_{32}Cl_3N_4O_{10}Dy$
M (g mol^{-1})	728.08	729.75	733.33
Crystal system	Triclinic	Triclinic	Triclinic
Space group	*P-1*	*P-1*	*P-1*
a (Å)	8.8714(5)	8.8490(18)	8.8460(18)
b (Å)	11.1470(6)	11.157(2)	11.148(2)
c (Å)	14.5317(8)	14.564(3)	14.527(3)
α (°)	102.922(3)	103.13(3)	102.85(3)
β (°)	93.887(2)	93.56(3)	93.52(3)
γ (°)	91.677(2)	91.72(3)	91.86(3)
V (Å^3)	1395.96(13)	1396.1(5)	1392.5(5)
T (K)	123(2)	100(2)	100(2)
Z	2	2	2
ρ_{calc} (g cm^{-3})	1.723	1.726	1.739
λ (Å)	0.71073	0.71090	0.71070
Data Measured	34764	28286	11894
Ind. reflns	8145	7446	5957
R_{int}	0.0252	0.1334	0.0560
Reflns with I > 2σ(I)	7464	7111	5850
Parameters	363	363	363
Restraints	12	12	12
R_1[a] (I > 2σ(I)), wR_2[a] (all data)	0.0232, 0.0518	0.0542, 0.1475	0.0330, 0.0844
goodness of fit	1.037	1.087	1.077
Largest residuals (e Å^{-3})	1.235, -0.911	3.944, -3.582	1.346, -1.452

[a] $R1 = \Sigma||F_o| - |F_c||/\Sigma|F_o|$, $wR2 = \{\Sigma[w(F_o^2-F_c^2)^2]/\Sigma[w(F_o^2)^2]\}^{1/2}$.

Table S2 – X-ray crystallographic data for 4 – 6.

	4	5	6
Formula	$C_{18}H_{32}Cl_3N_4O_{10}Ho$	$C_{18}H_{32}Cl_3N_4O_{10}Er$	$C_{18}H_{32}Cl_3N_4O_{10}Y$
M (g mol^{-1})	735.76	738.09	659.74
Crystal system	Triclinic	Triclinic	Triclinic
Space group	*P-1*	*P-1*	*P-1*

a (Å)	8.8700(18)	8.8067(5)	8.8190(18)
b (Å)	11.120(2)	11.1745(7)	11.149(2)
c (Å)	14.439(3)	14.5412(9)	14.491(3)
α (°)	102.36(3)	103.075(2)	102.91(3)
β (°)	93.95(3)	93.297(2)	93.47(3)
γ (°)	91.96(3)	91.942(2)	91.88(3)
V (Å^3)	1386.1(5)	1389.98(15)	1384.6(5)
T (K)	100(2)	123(2)	100(2)
Z	2	2	2
ρ_{calc} (g cm^{-3})	1.753	1.754	1.573
λ (Å)	0.71086	0.71073	0.71086
Data Measured	11497	20994	12146
Ind. reflns	5759	8118	6032
R_{int}	0.0291	0.0265	0.0176
Reflns with I > 2σ(I)	5461	7295	5719
Parameters	363	363	363
Restraints	12	12	12
R_1[a] (I > 2σ(I)), wR_2[a] (all data)	0.0282, 0.0747	0.0260, 0.0531	0.0339, 0.0936
goodness of fit	1.061	1.058	1.071
Largest residuals (e Å^{-3})	1.133, -1.705	0.883, -0.774	0.478, -0.971

[a] $R1 = \Sigma||F_o| - |F_c||/\Sigma|F_o|$, $wR2 = \{\Sigma[w(F_o^2-F_c^2)^2]/\Sigma[w(F_o^2)^2]\}^{1/2}$.

Table S3 – X-ray crystallographic data for 7 – 10.

	7	**8**	**9**	**10**
Formula	$C_{19}H_{24}N_7O_{14}Tb$	$C_{19}H_{24}N_7O_{14}Dy$	$C_{19}H_{24}N_7O_{14}Ho$	$C_{19}H_{24}N_7O_{14}Er$
M (g mol^{-1})	733.37	736.95	739.38	741.71
Crystal system	Monoclinic	Monoclinic	Monoclinic	Monoclinic
Space group	*P2$_1$/c*	*P2$_1$/c*	*P2$_1$/c*	*P2$_1$/c*
a (Å)	13.0909(18)	13.090(3)	13.0407(9)	13.0075(6)
b (Å)	14.851(3)	14.792(3)	14.8401(9)	14.8207(7)
c (Å)	13.916(2)	13.965(3)	13.9335(9)	13.9166(6)
α (°)	90	90	90	90
β (°)	102.875(4)	102.88(3)	102.721(2)	102.653(2)
γ (°)	90	90	90	90
V (Å^3)	2637.5(7)	2636.0(9)	2630.3(3)	2617.7(2)
T (K)	123(2)	100(2)	123(2)	123(2)
Z	4	4	4	4
ρ_{calc} (g cm^{-3})	1.847	1.857	1.867	1.882
λ (Å)	0.71073	0.71070	0.71073	0.71073
Data Measured	13733	23485	10968	26852
Ind. reflns	6777	6654	6231	7929
R_{int}	0.1060	0.0676	0.0603	0.0670
Reflns with I > 2σ(I)	4551	5539	4369	5503
Parameters	382	385	385	385
Restraints	10	5	5	5

R_1[a] (I > 2σ(I)), wR_2[a] (all data)	0.1072, 0.2416	0.0449, 0.1182	0.0729, 0.1556	0.0419, 0.0849
goodness of fit	1.086	1.080	1.137	0.985
Largest residuals (e Å^{-3})	3.640, -4.874	1.742, -1.813	1.186, -1.019	0.961, -0.935

[a] $R1 = \Sigma||F_o| - |F_c||/\Sigma|F_o|$, $wR2 = \{\Sigma[w(F_o^2-F_c^2)^2]/\Sigma[w(F_o^2)^2]\}^{1/2}$.

Table S4 – X-ray crystallographic data for 11.

	11
Formula	$C_9H_{12}N_5O_{12}Y$
M (g mol^{-1})	471.15
Crystal system	Triclinic
Space group	*P-1*
a (Å)	7.4349(15)
b (Å)	10.630(2)
c (Å)	11.657(2)
α (°)	68.02(3)
β (°)	88.31(3)
γ (°)	87.44(3)
V (Å^3)	853.4(3)
T (K)	123(2)
Z	2
ρ_{calc} (g cm^{-3})	1.834
λ (Å)	0.71073
Data Measured	11508
Ind. reflns	4844
R_{int}	0.0552
Reflns with I > 2σ(I)	4093
Parameters	257
Restraints	4
R_1[a] (I > 2σ(I)), wR_2[a] (all data)	0.1005, 0.1708
goodness of fit	1.274
Largest residuals (e Å^{-3})	1.136, -3.089

[a] $R1 = \Sigma||F_o| - |F_c||/\Sigma|F_o|$, $wR2 = \{\Sigma[w(F_o^2-F_c^2)^2]/\Sigma[w(F_o^2)^2]\}^{1/2}$.

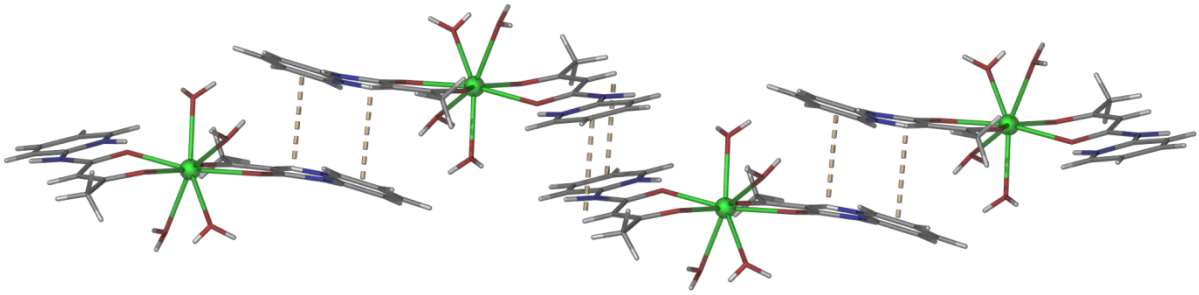

Figure S1 – π-π bonding along chains of 1 – 6.

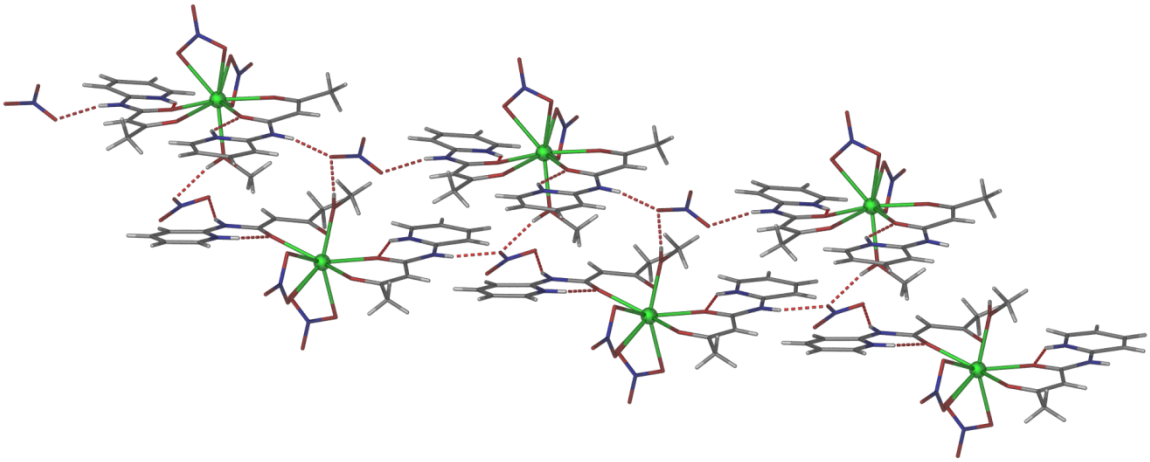

Figure S2 – Hydrogen bonding in a 'zipper' style between hydrogen bonded chains in 7 – 10.

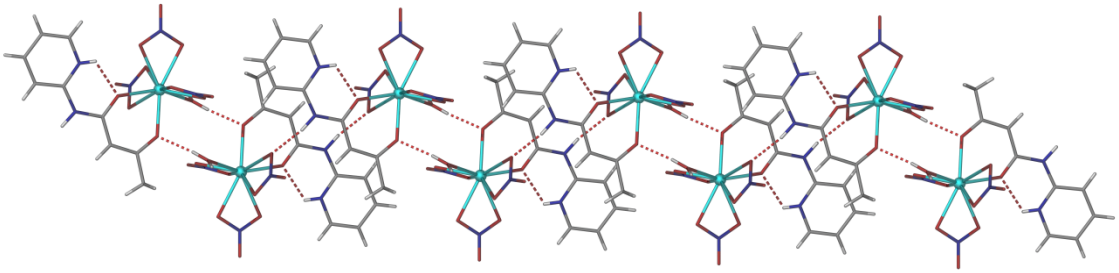

Figure S3 – Hydrogen bonding chains in 11.

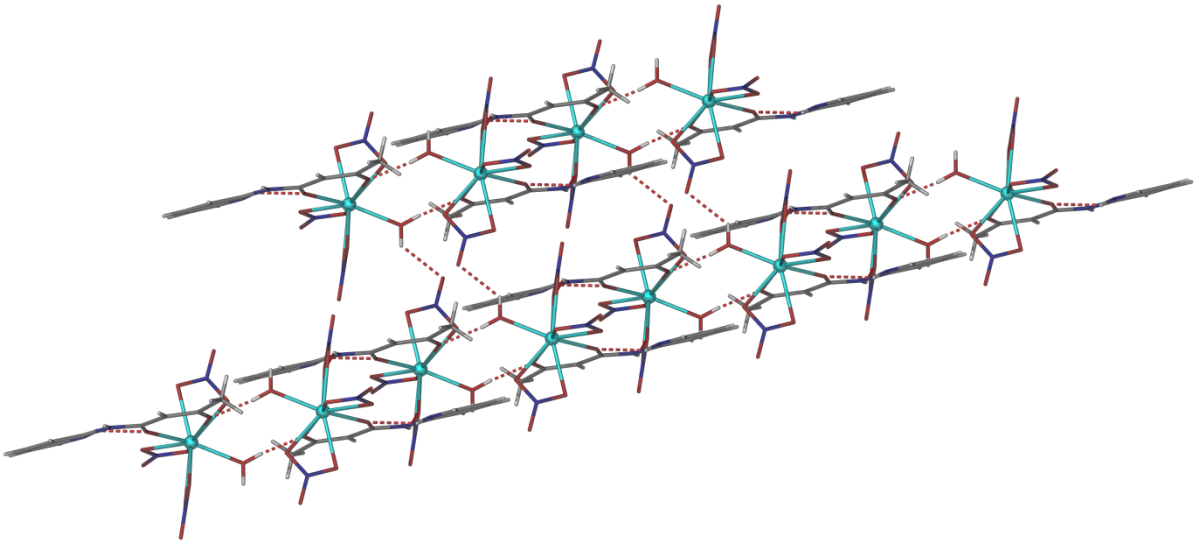

Figure S4 – Hydrogen bonding between the chains in 11 to form 2D sheets.

3. Magnetism

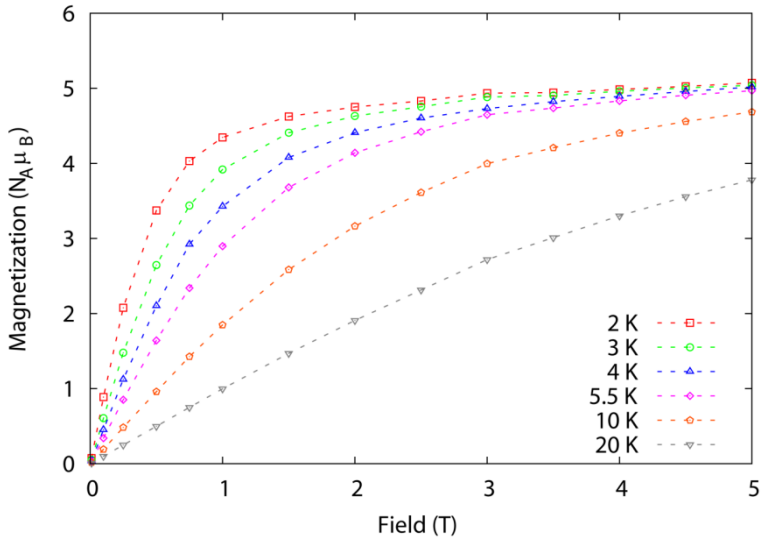

Figure S5 – Magnetization from 0 – 5 T at 2, 3, 4, 5.5, 10 and 20 K for 2.

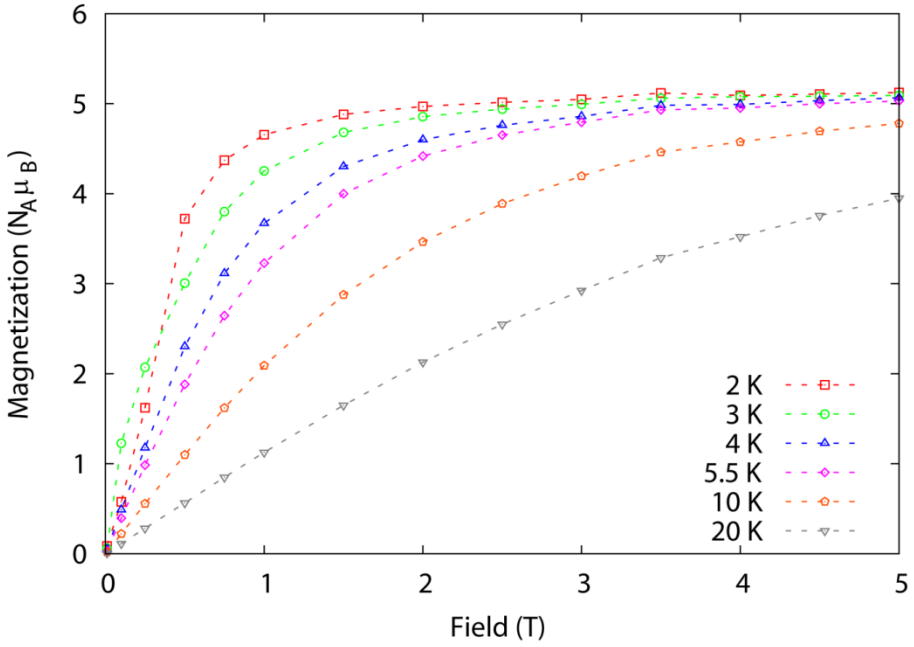

Figure S6 – Magnetization from 0 – 5 T at 2, 3, 4, 5.5, 10 and 20 K for 3.

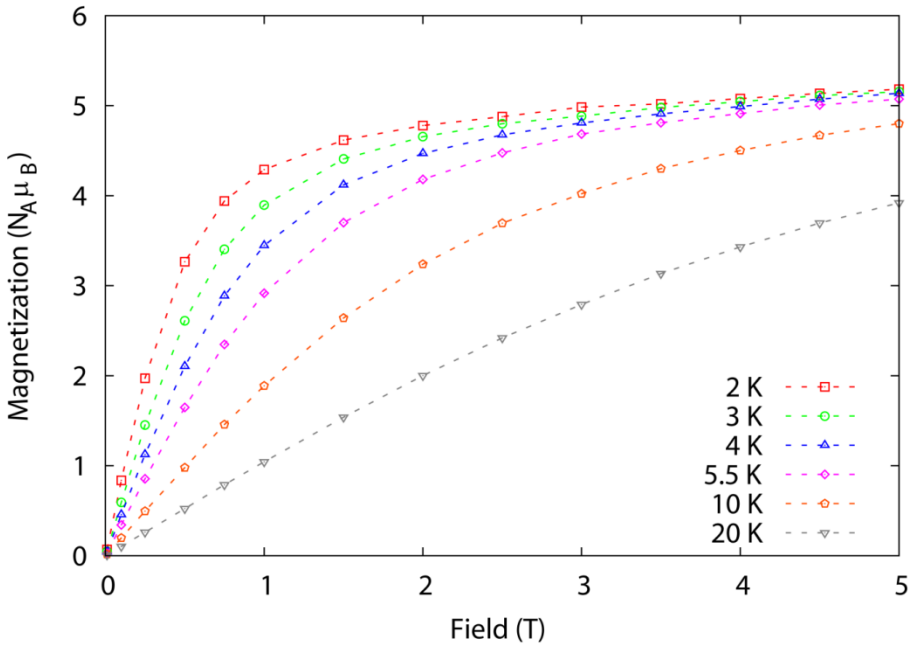

Figure S7 – Magnetization from 0 – 5 T at 2, 3, 4, 5.5, 10 and 20 K for 4.

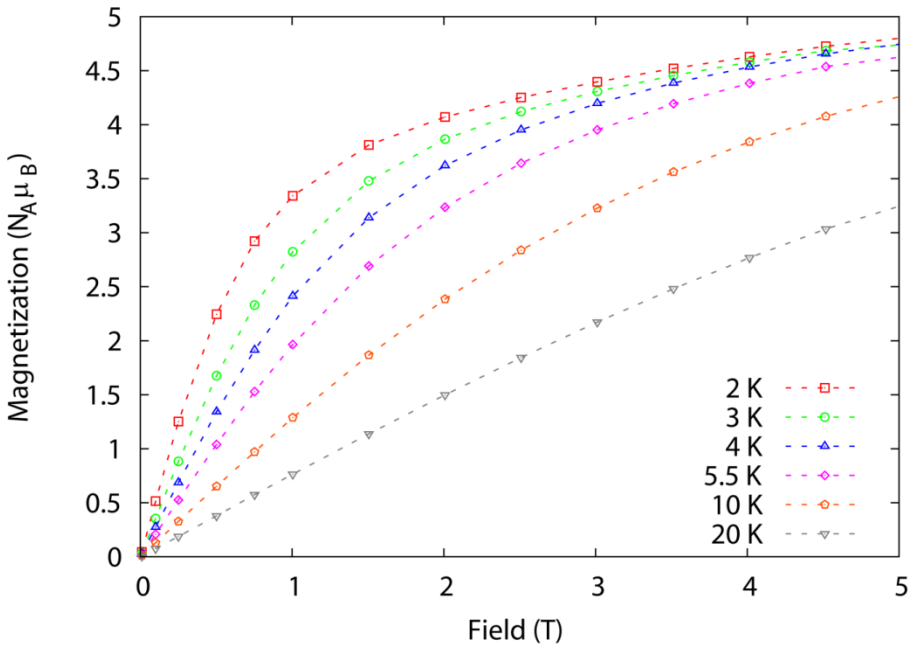

Figure S8 – Magnetization from 0 – 5 T at 2, 3, 4, 5.5, 10 and 20 K for 5.

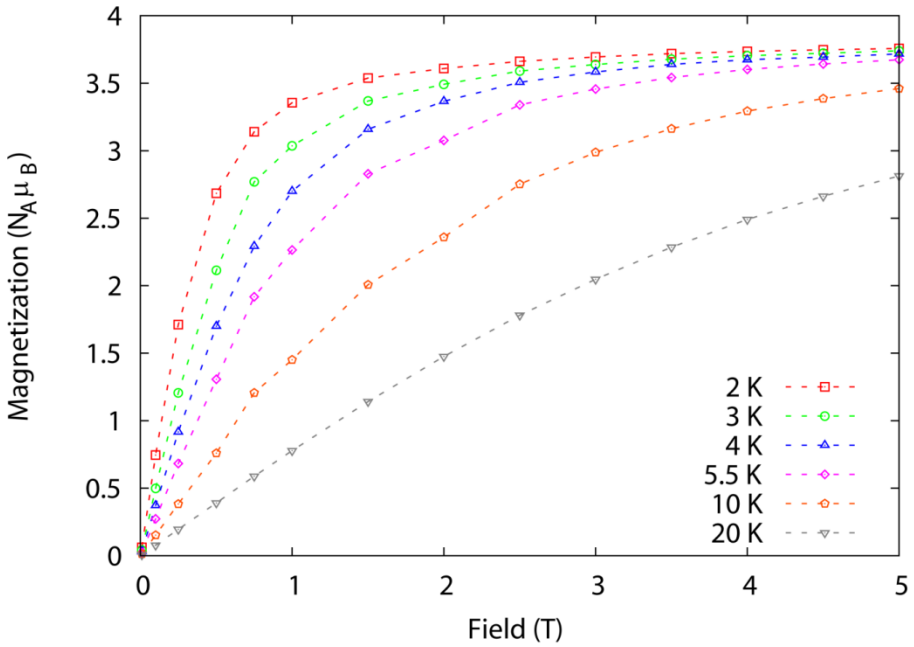

Figure S9 – Magnetization from 0 – 5 T at 2, 3, 4, 5.5, 10 and 20 K for 7.

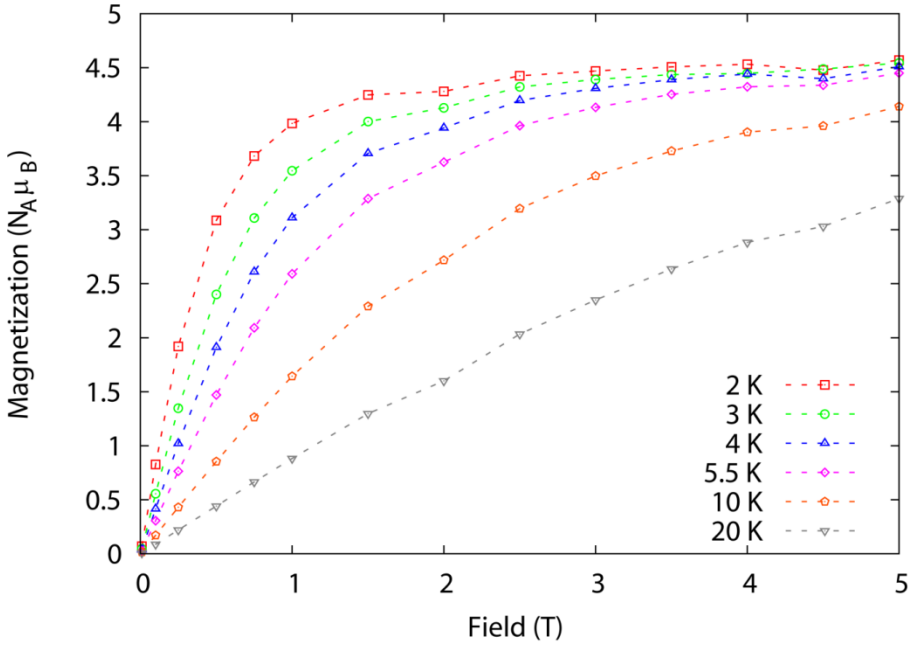

Figure S10 – Magnetization from 0 – 5 T at 2, 3, 4, 5.5, 10 and 20 K for 8.

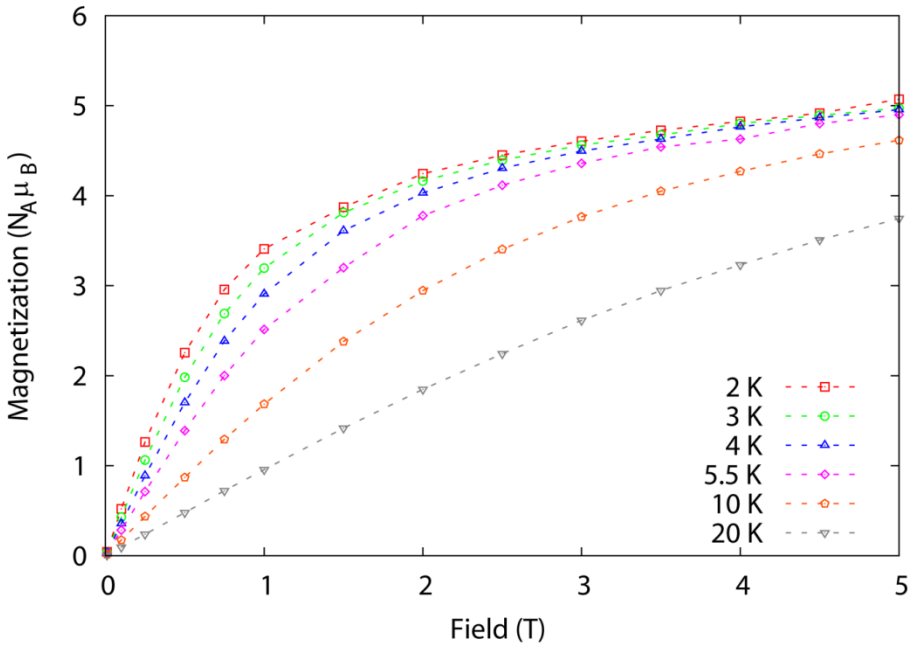

Figure S11 – Magnetization from 0 – 5 T at 2, 3, 4, 5.5, 10 and 20 K for 9.

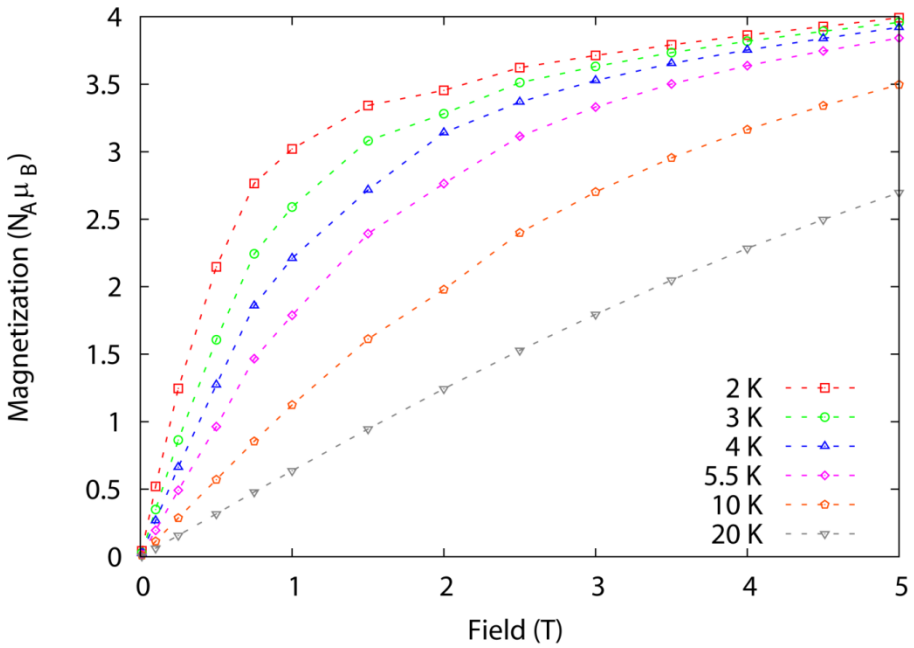

Figure S12 – Magnetization from 0 – 5 T at 2, 3, 4, 5.5, 10 and 20 K for 10.

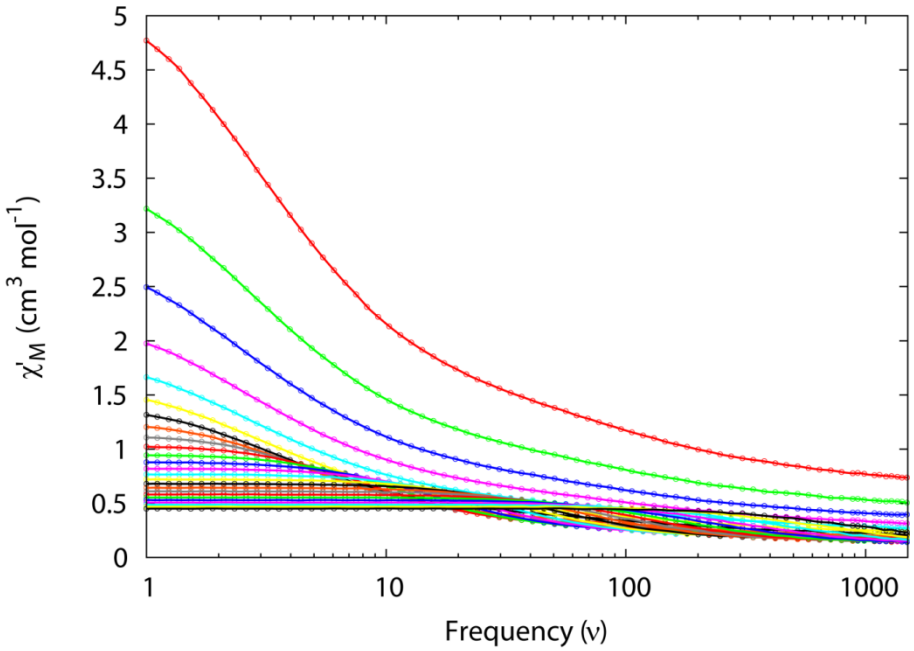

Figure S13 – In-phase AC magnetic susceptibility (χ_M') for 3 from 1 – 1500 Hz at temperatures from 2 – 26 K with 1 K intervals.

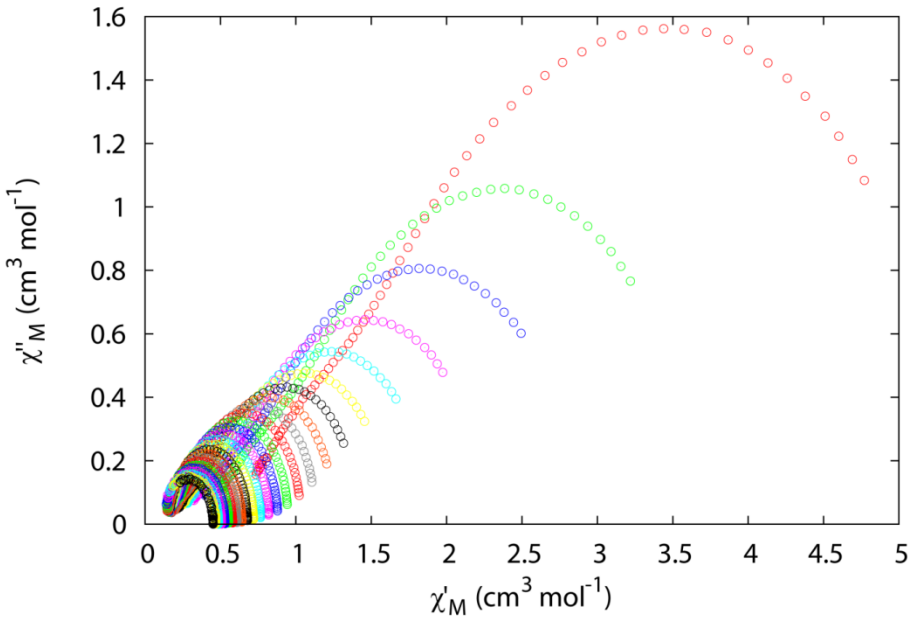

Figure S14 – Cole-Cole plot for 3 at temperatures of 2 K (top) to 26 K (bottom).

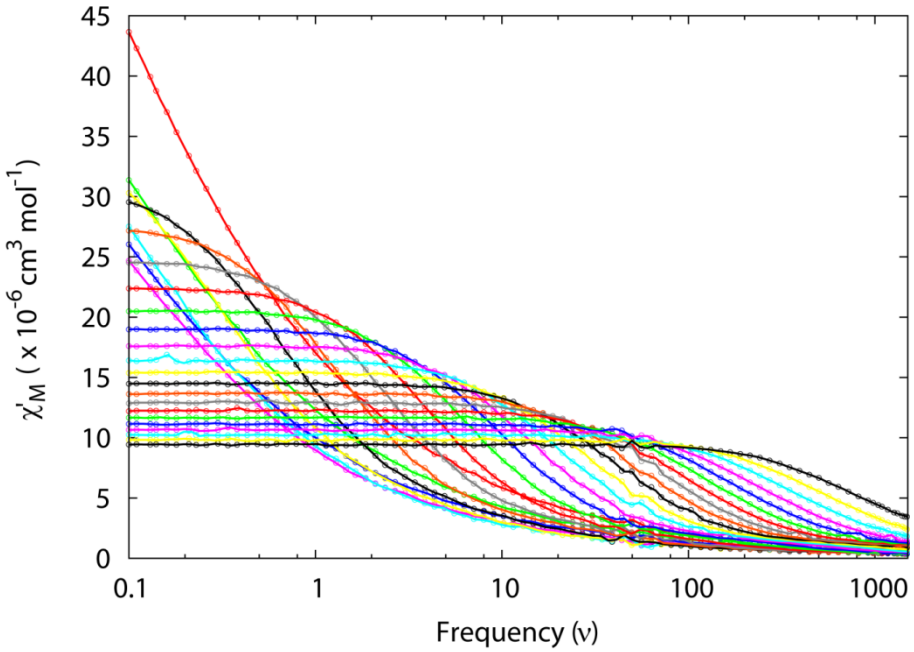

Figure S15 – In-phase AC magnetic susceptibility (χ_M') for 3:6 from 0.1 – 1500 Hz at temperatures from 2 – 26 K with 1 K intervals.

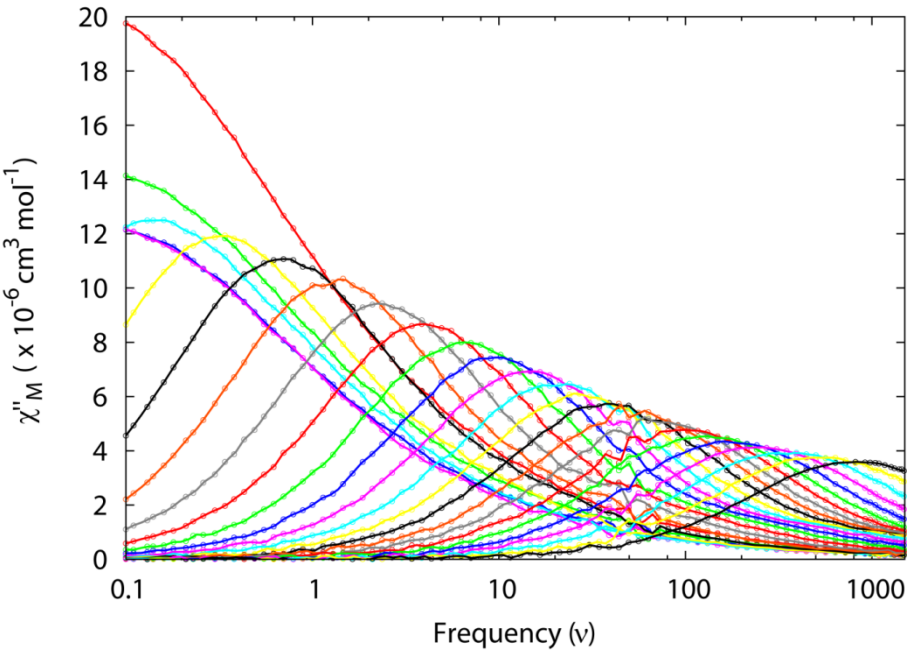

Figure S16 – Out-of-phase AC magnetic susceptibility (χ_M'') for 3:6 from 0.1 – 1500 Hz at temperatures from 2 – 26 K with 1 K intervals.

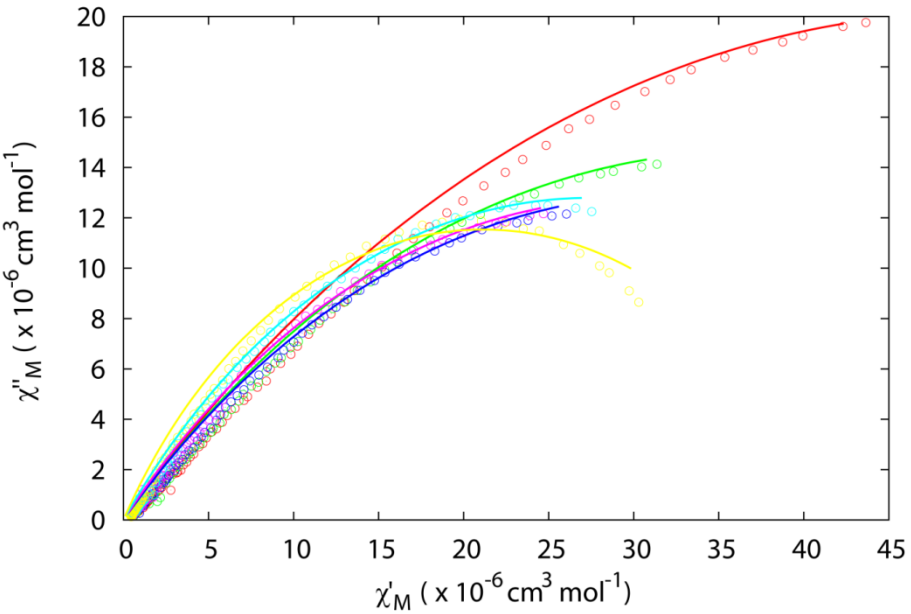

Figure S17 – Cole-Cole plot for 3:6 at temperatures of 2 K (top) to 7 K (bottom). Solid lines are fits to the modified Debye equation.

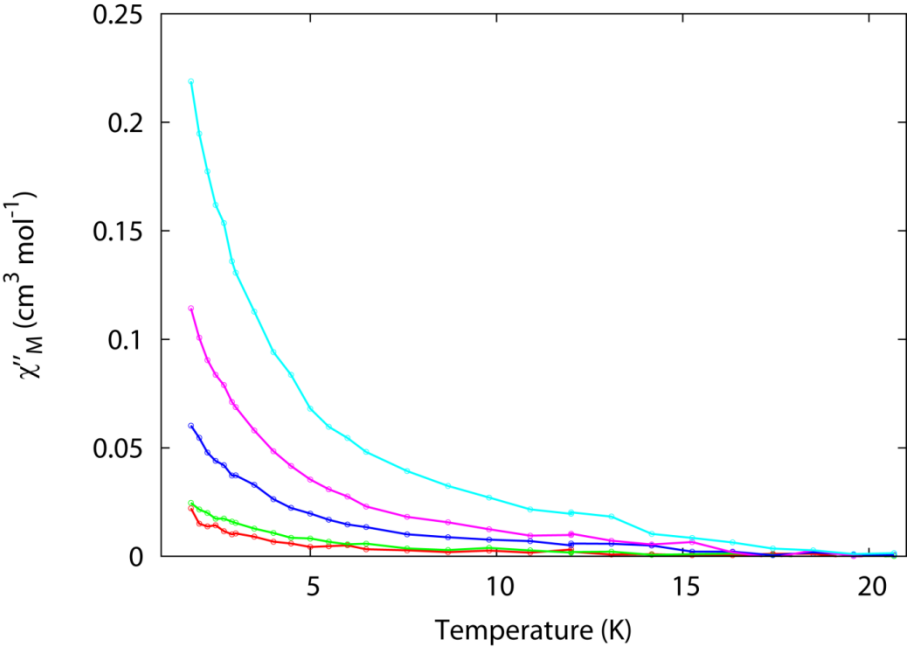

Figure S18 – Out-of-phase AC magnetic susceptibility (χ_M'') for 8 from 2 – 21 K at 50, 100, 250, 500 and 1000 Hz with zero DC field.

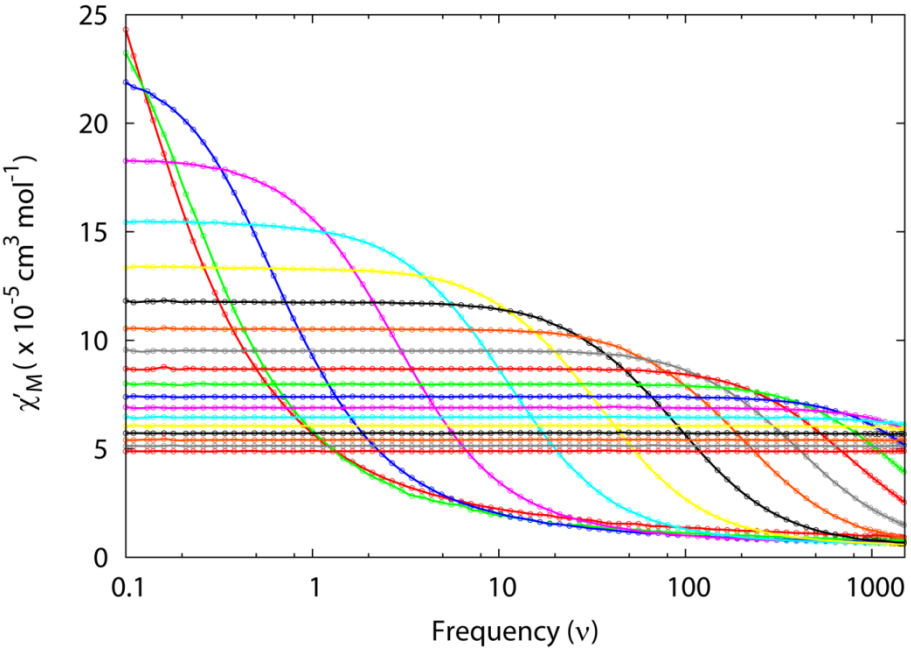

Figure S19 – In-phase AC magnetic susceptibility (χ_M') for 8 from 0.1 – 1500 Hz at temperatures from 2 – 20 K with 1 K intervals, in an 0.2 T DC field.

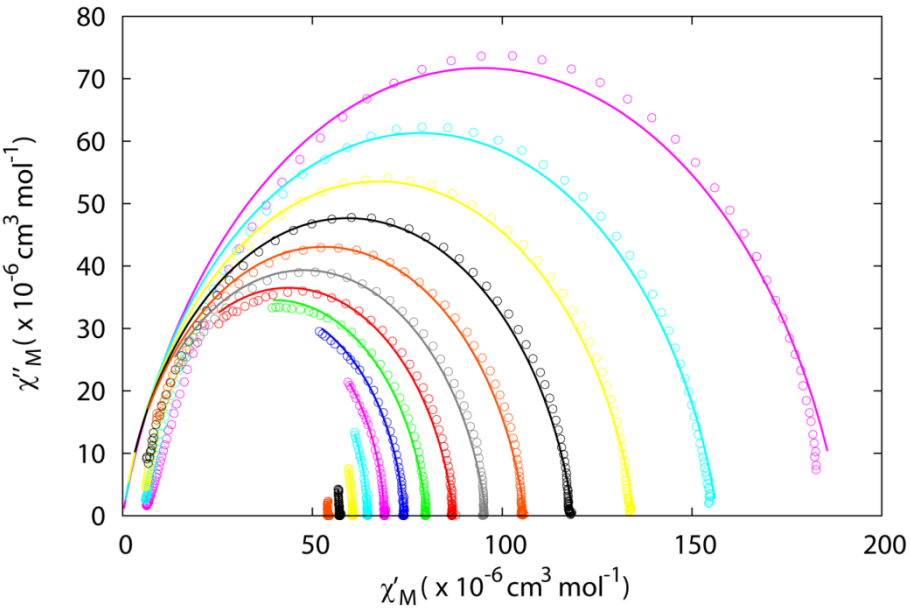

Figure S20 – Cole-Cole plot for 8 at temperatures of 5 K (top) to 18 K (bottom) in a field of 0.2 T. Solid lines are fits to the modified Debye equation.

4. Computational Details

The ANO-RCC-VTZP, VTZ and VDZ basis sets were used for the lanthanide ions, the first coordination sphere oxygen atoms and all other atoms, respectively. The calculations employed the second order Douglas-Kroll-Hess Hamiltonian, where scalar relativistic contractions are taken into account in the basis set and the spin-orbit coupling is handled separately in the RASSI module. CASPT2 corrections for dynamic electron correlation were not performed due to computational cost. The *g*-tensors for the Kramers doublets of Dy^{III} and Er^{III} and those for the pseudo-doublets of Tb^{III} and Ho^{III} were calculated based on the pseudo-spin $\tilde{S} = \frac{1}{2}$ formalism in the RASSI and SINGLE-ANISO modules. Note that for non-Kramers ions, g_x and g_y are necessarily equal to zero in the pseudo-spin $\tilde{S} = \frac{1}{2}$ formalism, due to vanishing off-diagonal matrix elements between the conjugate states.[6]

The active space for $[Tb(paaH^*)_2(H_2O)_4][Cl]_3 \cdot 2H_2O$, **2**, was 8 in 7 for the f^8 configuration of Tb^{III}. In the CI procedure, the septets were given 7 roots, the quintets were given 140 roots and the triplets were given 195 roots. The singlet states were not included due to computational limitations. In the RASSI module all 7 septets, 105 quintets and 112 triplets were mixed by spin-orbit coupling. Cholesky decomposition of the two-electron integrals was performed to save disk space. The splitting pattern of the electronic energy levels suggests six doublets and one singlet (level 9) and therefore the g_z values for the doublets were calculated.

The active space for $[Dy(paaH^*)_2(H_2O)_4][Cl]_3 \cdot 2H_2O$, **3**, was 9 in 7 for the f^9 configuration of Dy^{III}. In the CI procedure, the sextets were given 21 roots, the quartets were given 224 roots and the doublets were given 158 roots. In the RASSI module, 21 sextets, 128 quartets and 130 doublets were mixed by spin-orbit coupling.

The active space for $[Ho(paaH^*)_2(H_2O)_4][Cl]_3 \cdot 2H_2O$, **4,** was 10 in 7 for the f^{10} configuration of Ho^{III}. In the CI procedure, the quintets were given 35 roots, the triplets were given 210 roots and the singlets were given 196 roots. In the RASSI module, 30 quintets, 99 triplets and 31 singlets were mixed by spin-orbit coupling. The splitting pattern of the electronic energy levels suggests six doublets and five singlets (levels 5, 6, 7, 12 and 13) and therefore the g_z values for the doublets were calculated.

The active space for $[Er(paaH^*)_2(H_2O)_4][Cl]_3 \cdot 2H_2O$, **5**, was 11 in 7 for the f^{11} configuration of Er^{III}. In the CI and RASSI procedures, the quartets were given 35 roots and the doublets were given 112 roots.

The active space for $[Dy(paaH^*)_2(NO_3)_2(MeOH)][NO_3]$, **8**, was 9 in 7 for the f^9 configuration of Dy^{III}. In the CI procedure, the sextets were given 21 roots, the quartets were given 224 roots and the doublets were given 158 roots. In the RASSI module, 21 sextets, 128 quartets and 130 doublets were mixed by spin-orbit coupling.

5. References

1. M. Khalifa, *Bull. Fac. Pharm., Cairo Univ.*, 1961, 149.
2. *SADABS, SMART and SAINT*+, Bruker AXS Inc., Madison, Wisconsin, USA, 2007.
3. T. M. McPhillips, S. E. McPhillips, H.-J. Chiu, A. E. Cohen, A. M. Deacon, P. J. Ellis, E. Garman, A. Gonzalez, N. K. Sauter, R. P. Phizackerley, S. M. Soltis, and P. Kuhn, *J. Synch. Rad.*, 2002, **9**, 401–406.
4. W. Kabsch, *J. Appl. Cryst.*, 1993, **26**, 795–800.
5. G. M. Sheldrick, *Acta Cryst. A*, 2007, **64**, 112–122.
6. A. Abragam and B. Bleaney, *Electron Paramagnetic Resonance of Transition Ions*, Oxford University Press, 1970.